

Size-Luminosity scaling and Inverse Compton Seed Photons in Blazars

Markos Georganopoulos and John G. Kirk

*Max Planck Institut für Kernphysik, Postfach 10 39 80, D-69029,
Heidelberg, Germany*

Apostolos Mastichiadis

*Department of Astronomy, University of Athens, GR 15784, Athens,
Greece*

Abstract. We present preliminary results of our work on blazar unification. We assume that all blazars have a broad line region (BLR) and that the size of the BLR scales with the power of the source in a manner similar to that derived through reverberation mapping in radio quiet active galactic nuclei (AGNs). Using a self-consistent emission model that includes particle acceleration we show that according to this scaling, in weak sources like MKN 421, the inverse Compton (IC) scattering losses are dominated by synchrotron-self Compton scattering (SSC), while in powerful sources, like 3C 279, they are dominated by external Compton (EC) scattering of BLR photons. In agreement with other workers, we show that even in the powerful sources that are dominated by EC scattering, the hard X-ray emission is due to SSC. Finally, we show that this scaling reproduces well the observed sequence of blazar properties with luminosity.

1. Introduction

Blazars have been shown to exhibit a sequence of properties as a function of source power (Fossati et al. 1998). As the source power increases, the emission line luminosity and the ratio of Compton to synchrotron luminosity increase, while the synchrotron peak frequency ν_s and the IC peak frequency decrease. Recent multiwavelength studies support this scheme (e.g. Kubo et al. 1998), although the result that the ratio of the Compton to synchrotron luminosity increases with source luminosity suffers from limited statistics, and should be only considered tentative.

The initial division of blazars into flat spectrum radio quasars (FSRQs) and BL Lacertae objects (BLs) was based on the equivalent width (EW) of the broad emission lines. Sources with $EW > 5 \text{ \AA}$ were classified as FSRQs and sources with $EW < 5 \text{ \AA}$ as BLs. This difference in the EW of the emission lines has been interpreted as absence of a substantial BLR in BLs, and has been used to advance the idea that in BLs the GeV-TeV emission is due to SSC, while in FSRQs the GeV emission is due to EC. However, the EW criterion does not

correspond to a dichotomy (Scarpa & Falomo 1997), because a weak BLR is present in BLs as well. Additionally, it is not the BLR luminosity L_B that is relevant for the EC luminosity, but the BLR photon energy density U_E that is measured in the comoving frame of the non-thermal source. One needs to know not only L_B , but also the BLR radius R_B and the location of the non-thermal emitter relative to the BLR in order to quantify the relative importance of SSC versus EC emission.

The size of the BLR has been measured only for radio quiet AGNs through reverberation mapping (Kaspi et al. 2000), and it has been found to scale with the ionizing luminosity L_{acc} of the accretion disk as $R_B \propto L_{acc}^{0.7}$. It was additionally found that, assuming Keplerian motions for the BLR clouds, the mass of the central object scales with the ionizing luminosity as $M \propto L_{acc}^{0.5}$.

Here we assume the scalings apply also to radio loud AGN and examine the implications for blazars. Following the formalism of internal shocks propagating in a conical jet (Rees 1978), we scale the location D_{blob} and the radius R_{blob} of the non-thermal spherical emitter with the mass M of the central object. We assume that L_B is a fraction of L_{acc} and scale the kinetic luminosity and the Poynting flux of the blob with L_{acc} .

2. The scaling and its application

Under this scheme, the radius of the BLR scales as $R_B \propto L_{acc}^{0.7}$, and the distance of the blob from the center of the system scales as $D_{blob} \propto M \propto L_{acc}^{0.5}$. Therefore, we assume that for powerful sources the blob radiates from inside the BLR, $D_{blob} < R_B$. However, if we consider increasingly weaker sources, R_B falls faster than D_{blob} and, below some critical luminosity, the blob radiates from outside the BLR. For a blob inside the BLR, $U_E \propto (L_B/R_B^2)\Gamma^2$, where Γ is the bulk motion Lorentz factor of the blob. For a blob outside the BLR, the solid angle subtended by the BLR, as seen by the blob, is reduced. This affects U_E in two ways. The first is the usual geometric $1/r^2$ factor, and the second is a relativistic de-boosting that, for $D_{blob} \gg R_B$, gives $U_E \propto (L_B/D_{blob}^2)/\Gamma^2$ (Dermer & Schlickeiser 1994). The second effect dominates if the blob is located less than a few R_B away from the BLR. For example, for $\Gamma = 10$, U_E at a distance of $10 R_B$ is smaller than U_E inside the BLR by a factor of 10^2 due to the usual $1/r^2$ and by a factor of $\approx 10^4$ due to relativistic de-boosting.

We apply this scaling using a model (Georganopoulos & Kirk 2000) for the blob which includes both particle acceleration and radiative losses with IC scattering losses treated in the Thomson regime. Particles are accelerated in an acceleration zone and escape into a radiation zone, before they eventually escape out of the system.

This simplified picture is intended to represent particles which are accelerated by a shock front, escape it, and radiate downstream before the compressed plasma re-expands. Whilst undergoing acceleration, particles simultaneously suffer synchrotron losses and losses by Compton scattering of both photons of external origin (EC) and synchrotron photons (SSC) from the radiation zone. In the radiation zone, EC, SSC and synchrotron losses occur until the particle finally escapes after a time $t_{esc} = 3R_{blob}/c$. The electron energy distribution (EED) is computed self-consistently, taking account of these processes.

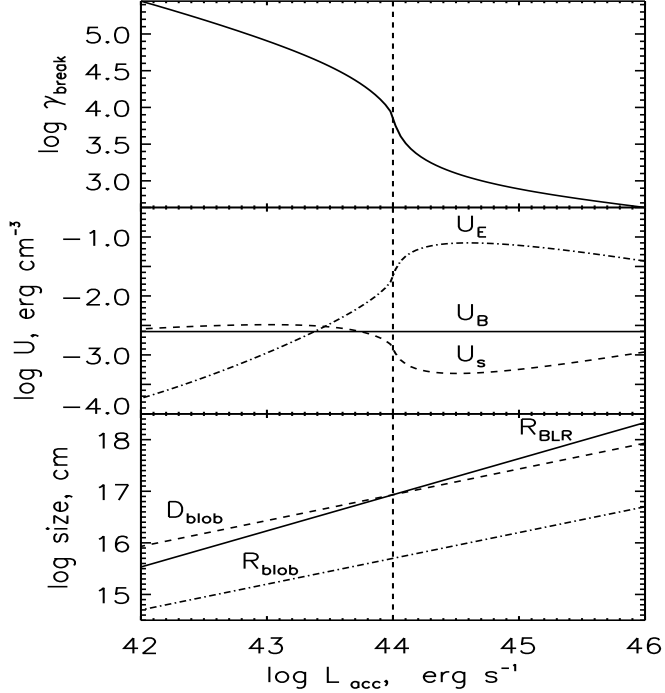


Figure 1. Sizes (lower panel), energy densities (middle panel), and the break of the EED as a function of the accretion disk luminosity.

Our assumption about the scaling of the Poynting flux implies a constant magnetic field, which we take to be $B = 0.2$ G. The blob is assumed to move with a Lorentz factor $\Gamma = 15$ at an angle $\theta = 1/\Gamma$ with respect to the line of sight. Low energy particles ($\gamma_0 = 10$) are injected into the blob at a rate of $Q = 0.1 \text{ cm}^{-3} \text{ s}^{-1}$. Also $L_B = 0.01 L_{acc}$. For $L_{acc} = 10^{44} \text{ erg s}^{-1}$, reverberation mapping gives $R_B \approx 8.6 \cdot 10^{16} \text{ cm}$. We assume that at this luminosity $R_B = D_{blob}$ and $R_{blob} = 2 \cdot 10^{15} \text{ cm}$.

In Fig.1, we let L_{acc} vary from $10^{42} \text{ erg s}^{-1}$ to $10^{46} \text{ erg s}^{-1}$, and follow the behavior of the system. In the lower panel R_B , D_{blob} , and R_{blob} are plotted as a function of L_{acc} . For weak sources, the blob is located outside the BLR ($D_{blob} > R_B$). As the source power increases, the blob gradually approaches and eventually enters the BLR. In the middle panel of Fig.1 we see how this affects U_E (the magnetic field energy density U_B is constant under the adopted scaling). For weak sources, U_E is much smaller than both U_B and the self-consistently derived synchrotron photon density U_S . Gradually U_E increases, and eventually, for bright sources, dominates over both U_B and U_S . In the upper panel of Fig.1 we plot the self-consistently derived break γ_{break} in the EED. Note that γ_{break} decreases as the power of the source decreases.

In Fig.2 we plot basic observable quantities as a function of L_{acc} . In the lower panel we plot the synchrotron luminosity L_S , the SSC luminosity L_{SSC} ,

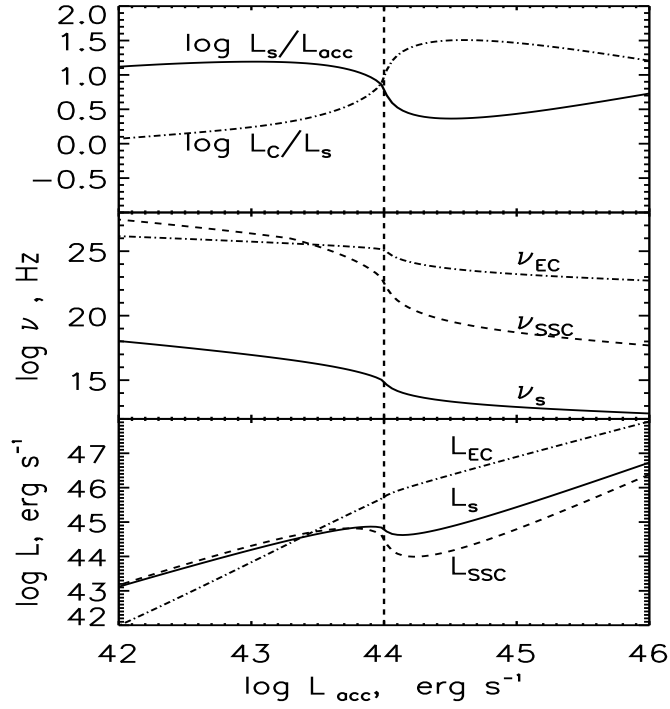


Figure 2. Luminosities (lower panel), peak frequencies (middle panel) and the ratio of synchrotron to accretion disk luminosity and IC to synchrotron luminosity (upper panel).

and the EC luminosity E_{EC} . At low powers, L_{EC} is much weaker than L_{SSC} and L_S that are roughly equal. As the source power increases, L_{EC} gradually dominates over L_{SSC} and L_S , and we end up with an EC dominated source. In the middle panel we plot the peak frequencies of the three emission components. Note how the synchrotron peak frequency ν_S decreases as the source power increases. Similar behavior is also seen for the SSC peak frequency ν_{SSC} and the EC peak frequency ν_{EC} . Finally in the upper panel of Fig.1 we plot the ratio L_S/L_{acc} (solid line) of the synchrotron to accretion disk luminosity and the ratio L_C/L_S of the IC luminosity to synchrotron luminosity. L_S dominates over L_{acc} in weak sources in agreement with the lack of a thermal component and weak emission lines in weak sources like BLs. L_{acc} becomes more significant for powerful sources, again in agreement with the strong emission lines of FSRQs and the accretion disk signature observed in some FSRQs (e.g. in 3C 279, Pian et al 1999). The dominance of the Compton over the synchrotron emission increases as the source power increases, in agreement with observations (e.g. Kubo et al. 1998). Note, however, that the observational case for an increasing Compton dominance with source power is based on poor statistics due to the limited sensitivity of the *CGRO*.

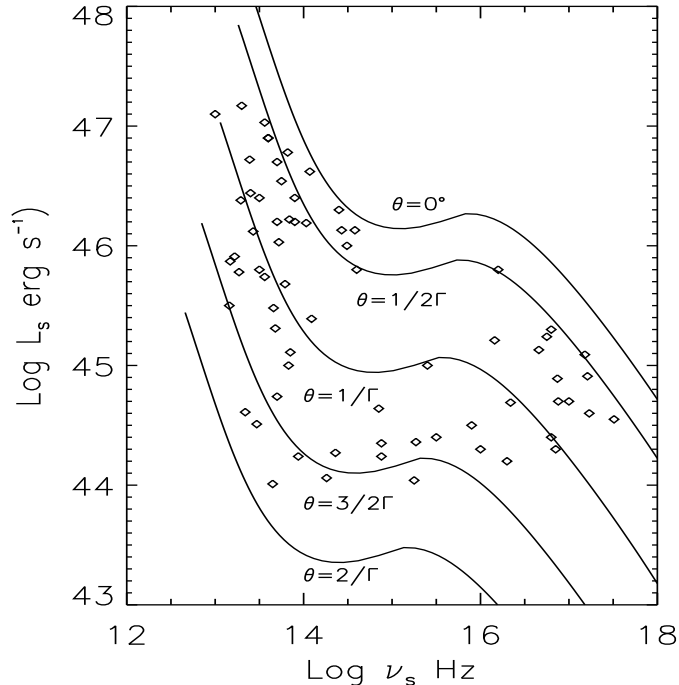


Figure 3. Synchrotron luminosity versus synchrotron peak frequency for a set of blazars (Sambruna et al. 1996, Kubo et al. 1998). Overlaid are the the model tracks as a function of L_{acc} for a range of observing angles.

In Fig.3 we plot the synchrotron luminosity L_s versus the synchrotron peak frequency ν_s for the blazars studied by Sambruna, Maraschi & Urry (1996) and Kubo et al. (1998). On top of the data points we plot the model tracks as a function of L_{acc} for a range of observing angles. Note that these tracks represent two model derived quantities, L_S and ν_S as L_{acc} varies. The model covers rather well the observed parameter space. Given the track of the model under an angle $\theta = 0^\circ$, we do not expect that any powerful ($L_S \approx 10^{47}$ erg s $^{-1}$) sources with high peak frequencies $\nu_S \approx 10^{17}$ Hz exist. The discovery of such sources would pose a serious problem for this model.

3. The luminosity scaling

In Fig.4 we plot the peak luminosities of the three emission mechanisms for 5 model sources with L_{acc} ranging from 10^{42} up to 10^{46} erg s $^{-1}$. The behavior of the model is in good agreement with the general characteristics of the observed luminosity sequence (compare with Fig.12 of Fossati et al. 1998). The synchrotron peak frequency decreases from 10^{18} Hz down to 10^{12} Hz, as the

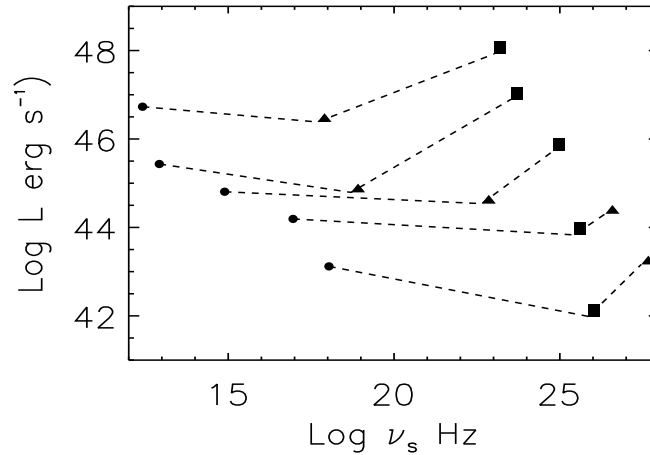


Figure 4. The model luminosity sequence. The synchrotron (circles), SSC (triangles), and EC (squares) luminosity as a function of frequency for 5 model sources of different intrinsic power. The broken lines link points from a single model.

synchrotron power increases. The Compton peak frequency in weak sources is in the TeV regime ($\approx 10^{25-26}$ Hz) and it is due to SSC, while in powerful sources it is in the GeV regime ($\approx 10^{23}$ Hz) and it is due to EC. According to the model, although in these bright sources the energy losses are dominated by EC, the hard X-ray emission is due to SSC, in agreement with recent observations (Kubo et al. 1998).

We note here that Fig.4 corresponds to sources that are oriented at an angle $\theta = 1/\Gamma$. In reality one should expect a range of angles, which will give rise to significant scattering around the presented trend. This scattering is visible in the work of Fossati et al. (1998) and indicates that a proper unification scheme for blazars should include the effects of orientation.

References

- Dermer, C. D., & Schlickeiser, R. 1994, *ApJS*, 90, 945
 Fossati, G., et al. 1998, *MNRAS*, 299, 433
 Georganopoulos, M. & Kirk, J.G. 2000, in preparation
 Kaspi, S., et al. 2000, *ApJ*533, 631
 Kubo, H., et al. 1998, *ApJ*, 504, 693
 Pian, E. et al. 1999, *ApJ*, 521, 112
 Rees, M.J. 1978, *MNRAS*, 184, 61
 Sambruna, R. M., Maraschi, L., & Urry, C. M. 1996, *ApJ*, 463, 444
 Scarpa, R., Falomo, R. 1997, *A&A*, 325, 109